Available online at www.sciencedirect.com
ScienceDirect
International Journal of Multiphase Flow 34 (2008) 665–677
International Journal of Multiphase Flow
www.elsevier.com/locate/ijmulflow

On the phase inversion process in an oil–water pipe flow

K. Piela [a], R. Delfos [a], G. Ooms [a,*], J. Westerweel [a], R.V.A. Oliemans [b]

[a] J.M. Burgerscentrum, Delft University of Technology, Laboratory for Aero- and Hydrodynamics, Leeghwaterstraat 21, 2628 CA Delft, The Netherlands
[b] J.M. Burgerscentrum, Delft University of Technology, Kramers Laboratorium, Prins Bernhardlaan 6, 2628 BW Delft, The Netherlands

Received 10 October 2007; received in revised form 3 December 2007

Abstract

An experimental study of the phase inversion process in an oil–water flow through a pipe was carried out. Special attention was paid to the critical concentration of the dispersed phase at which phase inversion occurs and to the change in morphological structures during inversion. To that purpose two different types of experiments were performed: (1) continuous experiments during which the dispersed phase fraction was gradually increased and (2) direct experiments whereby oil and water were injected simultaneously into the pipe at a certain concentration. During the experiments detailed pictures were taken of the phase inversion process and simultaneously the electrical conductivity of the mixture was measured to determine which liquid formed the continuous phase and which the dispersed phase. Also the pressure gradient over several parts of the pipe was measured.

For continuous experiments the critical concentration was found to depend on the injection phase volume fraction. The critical concentration was significantly higher for continuous experiments than for direct experiments. The change in morphological structures during phase inversion was the same for the two types of experiments. During inversion the concentration of drops of the (originally) dispersed phase becomes so high, that they coalesce at certain places in the flow field and form relatively large, rather complex, morphological structures. With a further increase in concentration of the (originally) dispersed phase these morphological structures grow in size and start to form the new continuous phase in which again complex structures are present, but this time consisting of the (originally) continuous phase.

Keywords: Two-phase flow; Oil–water flow; Phase inversion; Horizontal pipe

1. Introduction

The flow of two immiscible liquids often occurs as a dispersed flow, where one liquid is present in the other liquid in the form of drops. Dispersions are widely used in the petrochemical-, food-, chemical- and pharmaceutical industries. Handling and controlling dispersion properties is of a key interest for practical applications. Special interest has to be given to the phase inversion phenomenon, whereby the dispersed phase becomes the continuous one, and vice versa. During this process the effective viscosity of the mixture becomes very large, which leads to high pressure drops or low flow rates.

The phase inversion phenomenon has been studied for many years (see, for instance, Becher, 2001), but there are still many questions about the inversion process. Some authors assume that a sudden coalescence of drops can encapsulate parts of the continuous phase, which causes drop formation from the (originally) continuous phase (Yeo et al., 2002; Brauner and Ullmann, 2002). Others observed the creation of multiple drops (small droplets of the continuous phase inside the drops) prior to inversion (Pacek et al., 1994; Pacek and Nienow, 1995; Pal, 1993; Sajjadi et al., 2000, 2002, 2003; Liu et al., 2005, 2006). According to some authors inversion is a rather rapid process, called catastrophic by them, (Dickinson, 1981; Smith

* Corresponding author. Tel.: +31 15 2781176; fax: +31 15 2782979.
E-mail address: G.Ooms@tudelft.nl (G. Ooms).

0301-9322/$ - see front matter © 2008 Elsevier Ltd. All rights reserved.
doi:10.1016/j.ijmultiphaseflow.2007.12.004

and Lim, 1990; Rondón-Gonzaléz et al., 2006; Tyrode et al., 2005; Vaessen et al., 1996; Binks and Lumsdon, 2000). However, during our experiments we found that this is not strictly true as also shown by Liu et al. (2006).

Most of the experiments reported in the literature were performed in a stirred vessel and usually water and oil were used. They were often continuous experiments during which the dispersed phase was gradually added to the continuous phase. For this type of experiments it was found, that phase inversion could be postponed to a high value (>0.8) of the dispersed phase volume fraction. Also a wide ambivalent volume fraction region existed where the mixture could be either water continuous or oil continuous (Vaessen et al., 1996; Groeneweg et al., 1998; Deshpande and Kumar, 2003; Mira et al., 2003; Tyrode et al., 2003). During direct experiments in a stirred vessel the two liquids were mixed at a certain concentration (Quinn and Sigloh, 1963; Tyrode et al., 2005) and inversion usually occurred at a value of the dispersed phase fraction close to 0.5 (dependent on the properties of the liquids) and no ambivalence region was observed.

It is important to point out, that in the above mentioned papers some are without an added surfactant (for instance Deshpande and Kumar, 2003; Pacek and Nienow, 1995; Liu et al., 2005, 2006) and others with an added surfactant (for instance Binks and Lumsdon, 2000; Rondón-Gonzaléz et al., 2006; Tyrode et al., 2005). The presence of a surfactant can have a significant influence on the inversion process; they tend to favor one type of dispersion over the other. In our experiments we have not added a surfactant. However, in the oil (that we used) there were small concentrations of substances that were acting like a surfactant, as water was favored as the continuous phase.

Only a few phase-inversion experiments were carried out in a pipe. Direct experiments were done by Liu et al. (2006) in a vertical pipe and by Pal (1993), Nädler and Mewes (1997), Ioannou et al. (2005) and Chakrabarti et al. (2006) in a horizontal pipe. They paid particular attention to the pressure drop increase during phase inversion. We performed continuous experiments in a horizontal pipe – see Piela et al. (2006). We measured also a strong increase in the pressure drop during the inversion process. Moreover we made pictures of the change in morphological oil–water structures during inversion. As for the stirred-vessel experiments the comparison between the direct experiments and the continuous experiments showed, that also in the case of a pipe flow the critical concentration of the dispersed phase fraction at inversion was very different for the two types of experiments. Dependent on the experimental conditions the critical concentration can be significantly higher for continuous experiments than for direct experiments. For practical applications this result is very important, as it opens the opportunity to avoid or postpone phase inversion (causing a high pressure drop or low flow rate) by gradual injection of the dispersed phase into the continuous one. Therefore we decided to carry out a new set of experiments to study the critical concentration for continuous experiments as function of some parameters (such as the injection phase volume fraction). To get additional information also detailed pictures were taken during phase inversion for both continuous and direct experiments. It is our hope and expectation, that the information about the dependence of the critical concentration on some relevant parameters and the detailed pictures of the structures occurring during phase inversion will lead to a better control of the phase-inversion process for practical applications.

The novelty of this publication beyond that of Piela et al. (2006) is: the comparison between continuous experiments and direct experiments, the detailed observation of the inversion process and the influence of the injection phase volume fraction on the width of the ambivalence region.

In Section 2 of this paper the experimental facilities used for the continuous and direct experiments are described. Then results from the continuous experiments are presented in Section 3 and from the direct experiments in Section 4. Section 5 describes in detail important interactions taking place during phase inversion. In Section 6 particular attention is paid to the ambivalence region and the critical concentration for continuous experiments. Finally, in Section 7 concluding remarks are made.

2. Experiments

2.1. General information

The details of the pipe configurations used for the two types of experiments will be given when these experiments are discussed. An acrylic pipe with an inner pipe diameter of 16 mm was used. The two immiscible liquids used were tap water and Shell Macron EDM 110 oil (density 794 kg/m^3, kinematic viscosity at 20° 3.9 mm^2/s and oil–water interfacial tension 0.045 N/m). All experiments were performed at high Reynolds and Froude numbers to make sure that always a fully dispersed flow was present (according to Brauner (2001) a mixture velocity of 1.35 m/s is sufficient for our experimental conditions). Under such conditions the slip velocity is negligible and the dispersed phase volume fraction could therefore directly be calculated from the measured density. In both types of experiments the mixture velocity in the pipe was kept constant.

To make a detailed study of the dispersion morphology samples were taken from the flow by means of a 7 mm inner diameter sampling tube and led through a visualization cell (which consists of 2 glass plates 1 mm apart; the length of the cell is 20 mm). The visualization cell was illuminated from one side with a 500 W halogen lamp and a high speed camera took images at the other side. The camera was operated at a frame rate of 50 Hz and 500 Hz. A sketch of the sampling technique is given in Fig. 1. To check whether this observation procedure had some influence on the dispersion morphology we performed experiments with various distances between the visualization

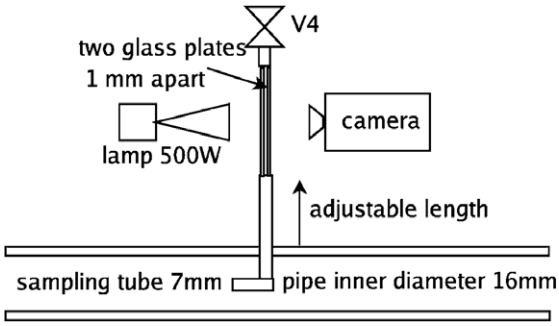

Fig. 1. Sketch of the visualization method.

cell and the pipe and with various sample flow rates . We always achieved the same results. We also changed the distance between the glass walls from 1 mm to 5 mm and again the results were the same.

Pressure drops were measured at different locations over a distance of 1 m. Differential pressure transducers (Validyne DP-15, measuring error <3%) were used and the pressure signal was sampled at a rate of 2 kHz. Data were averaged over 2000 samples. Conductivity measurements (at the same frequency) were done with a cell consisting of two (0.2 mm diameter) wire electrodes mounted in the pipe: one in the vertical direction and one in the horizontal direction. The distance between the electrodes in the center of the pipe was 2 mm. During the experiment we also monitored the temperature with a thermocouple mounted in the pipe wall. Most of the experiments were conducted more than two times and the reproducibility of the experiments was good.

2.2. Continuous experiments

The sketch of the set-up used for the continuous experiments is shown in Fig. 2. The symbols used in the sketches have the following meaning: V: valves, F1: Krohne Optimass 7000 flow meter (measuring error <0.26%), F2: Krohne Corimass E flow meter (measuring error <0.4%), C1: conductivity cell and T1: thermocouple. During the continuous experiments one of the liquids (water or oil) was taken from the continuous phase tank (see Fig. 2) and recirculated through the pipe loop by means of pump 1. Pump 1 is a positive displacement pump (lobe pump), chosen to minimize the pumping effect on the dispersion morphology. After recirculating the liquid for a few minutes to ensure that the pipe walls were wetted by the liquid, injection of the other liquid started by pumping (using pump 2) the dispersed phase through the injector into the pipe loop. During the injection valve 2 was opened and the same volume of dispersion liquid was removed from the pipe loop as the volume that was injected. Flow meter 1 measured the density and the flow rate of the mixture in the pipe loop. The flow meter was calibrated for oil–water mixtures. The mixture velocity was kept constant during the experiment by an electronic feedback system (pump 1 was controlled based on measurements of flow meter 1). To study the influence of the length of the pipe loop also continuous experiments were carried out, whereby the pipe loop was significantly reduced in length. During these experiments the mixture flows more often through the pump. However, we observed no difference in the results when compared with the results of the experiments carried out in the longer pipe loop.

A cylindrical container (placed around the pipe loop) with a number of holes in it was used as injector. The oil was pumped through the holes into the pipe loop. Three different types of injector were used, viz., a container with 2 holes of 2 mm diameter, a container with 8 holes of 2 mm diameter, and one with 100 holes of 3 mm diameter (for more details, see Piela et al., 2006). The experimental results were independent of the injector type. The pressure drop was measured just after the injector, 2 m (125d) downstream of the injector and 5 m (313d) downstream of it.

2.3. Direct experiments

During the direct experiments water and oil were taken from the two tanks and injected simultaneously by means of pump 1 and pump 3 into the pipe (see Fig. 3). The mixture was injected at a constant concentration for at least 40 s. Flow meter 1 measured the density and the flow rate of the mixture in the pipe. The oil volume fraction was calculated from the density measurement. The pressure drops were measured at six different positions: immediately downstream of the inlet and at distances of 2.0 m (125d), 5.0 m (313d), 11.7 m (731d), 18.7 m (1169d) and 26.5 m (1656d) from the inlet.

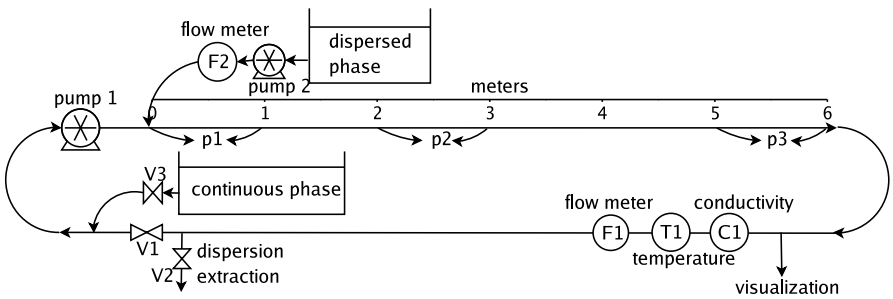

Fig. 2. Sketch of the experimental set-up for continuous experiments.

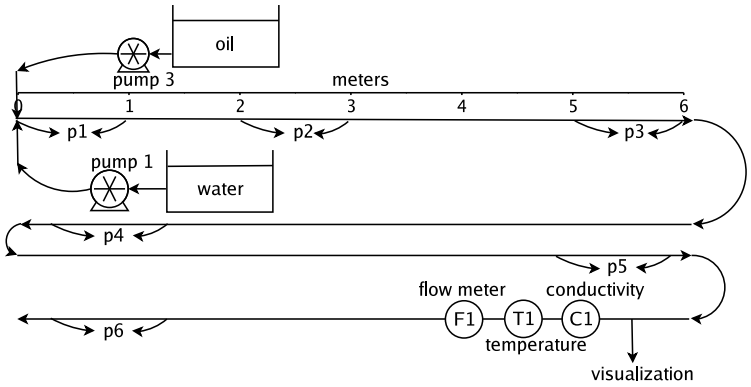

Fig. 3. Sketch of the experimental set-up for direct experiments.

3. Results for continuous experiments

A continuous experiment starts by flowing the first liquid at a certain velocity through the pipe loop and then gradually increasing the concentration of the second liquid by injecting it (in the form of drops) at a certain flow rate into the first liquid. In our description of the morphological structures we will use the following three terms: drops, pockets and regions. A drop is the smallest part of the dispersed phase, usually smaller than 1 mm. A pocket is a larger unit of one of the two phases, that contains several drops of the other phase (see Fig. 4); it is usually of the order of a few millimeters up to 1 cm. Finally a region is a still larger part of one of the two phases in the flow field, that encloses several pockets and drops of the other phase and is of the order of 1 cm or larger. In a few cases we will also use the term multiple drop, which is a drop containing small droplets of the other phase. A pocket is larger than a multiple drop and the surface tension is not strong enough to give the pocket a spherical shape, whereas a multiple drop is (nearly) spherical.

3.1. Phase-inversion mechanism

During a continuous experiment the dispersed phase fraction gradually increases and also the effective viscosity increases (see Pal, 2000). At a certain critical concentration of the dispersed phase inversion occurs. Fig. 4 shows the different stages of the phase-inversion process for a water-continuous flow to an oil-continuous flow (water-to-oil experiment) for a mixture velocity of 1 m/s and an injection phase volume fraction (ratio of the injection flow rate and the mixture flow rate in the pipe) of 0.125. The top-left picture shows the start of the inversion process at an oil volume fraction of 0.84. Some larger oil-continuous pockets (containing water droplets) are formed in a water-continuous region due to coalescence of the original oil drops. After 16 s (bottom-left picture) the number of these oil-continuous pockets has increased due to continuous oil injection via the injector. With further oil injection isolated water-continuous pockets are created embedded in oil-continuous regions. After 43 s (top-right picture) the oil-continuous pockets in water-continuous regions

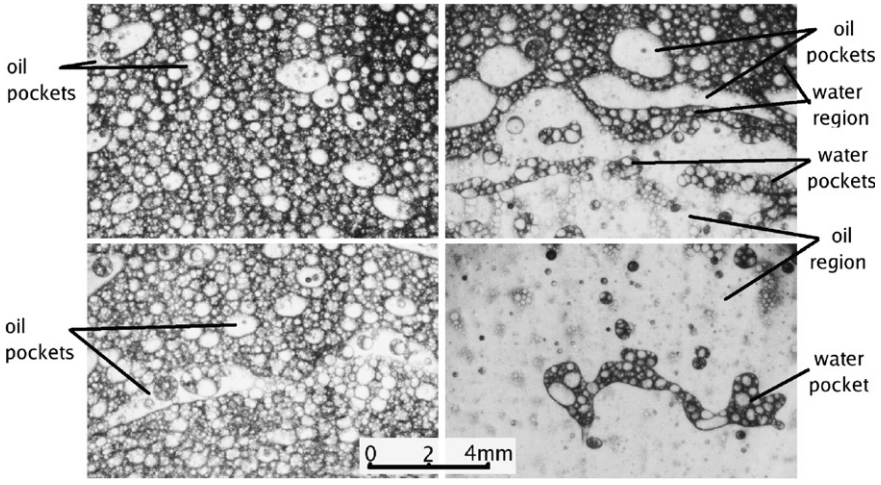

Fig. 4. Inversion from a water-continuous flow to an oil-continuous flow during a continuous experiment. Starting from the top-left picture, the bottom-left picture is taken after 16 s, the top-right after 43 s and bottom-right after 82 s.

and water-continuous pockets in oil-continuous regions are about the same in number and size. With further oil injection the oil-continuous pockets disappear and only water-continuous pockets in an oil-continuous region remain. After 82 s (bottom-right picture) the phase inversion is almost completed. There are still some isolated water-continuous pockets, that break-up into drops.

The phase-inversion process as described above does not take place at the same time at all locations in a cross-section of the pipe flow. This can clearly be observed in Fig. 5, which shows the complete side view of the pipe for a continuous experiment at a mixture velocity of 1 m/s and an injection phase volume fraction of 0.25. The top-left picture shows the dispersion before inversion. Because of the high oil volume fraction the dispersion is not transparent. After 6 s (center-left picture) the dispersion close to the pipe walls inverts (from water continuous to oil continuous) and the mixture becomes transparent in these regions (as the concentration of the dispersed phase is lower). After 22 s (bottom-left picture) inverted regions can also be observed in the center of the pipe. After 33 s (top-right picture) large non-inverted water-continuous regions are separated by the new oil-continuous phase. 4 s later the pump was stopped and non-inverted water-continuous regions settle to the bottom of the pipe due to their negative buoyancy (center-right picture). It can clearly be observed that the volume fraction of non-inverted (water-continuous) regions is still large. It takes another 39 s to get fully separated layers (bottom-right picture).

3.2. Dimensionless parameters

We made an attempt to describe phase inversion during the continuous experiments by means of dimensionless parameters. To that purpose we introduce four dimensionless groups, viz. the Reynolds number $Re = \frac{\rho u d}{\mu}$, the Froude number $Fr = \frac{u}{\sqrt{gd}}$, the Weber number $We = \frac{\rho u^2 d}{\sigma}$, and the injection phase volume fraction χ. ρ is the fluid density, u the average (mixture) velocity, d the pipe diameter, μ the kinematic viscosity, g the gravity acceleration and σ the water–oil surface tension.

In Fig. 6 the measured results for the friction factor $f = \frac{2\Delta P d}{\rho u^2 L}$ (ΔP is the pressure drop over a distance L) are given for water-to-oil continuous experiments at values of χ of 0.03, 0.125 and 0.18, as function of the dispersed phase volume fraction. (The values of Re, Fr and We at the start of these experiments are given in Table 1). As can be seen the friction factor increases with increasing dispersed phase volume fraction, until it reaches its maximum during phase inversion after which it decreases significantly. When we repeated these experiments for the same value of χ at different (but sufficiently large) velocities u (and hence different values of Re, Fr and We) the results did not change. Fig. 6 shows the significant influence of the injection phase volume fraction χ on the phase-inversion process. Both the dispersed phase volume fraction and the friction factor at the point of phase inversion depend on χ.

To study the dependence on the velocity with which the dispersed phase was injected into the mixture also water-to-oil continuous experiments were carried out for several values of the injection velocity at the same value of the injection phase volume fraction χ. This was achieved by using different numbers of holes in the injector. In Fig. 7 the friction factor for these experiments is given as function of dispersed phase volume fraction for three values of the injection velocity. It can be concluded that the friction factor and dispersed phase volume fraction at phase inversion

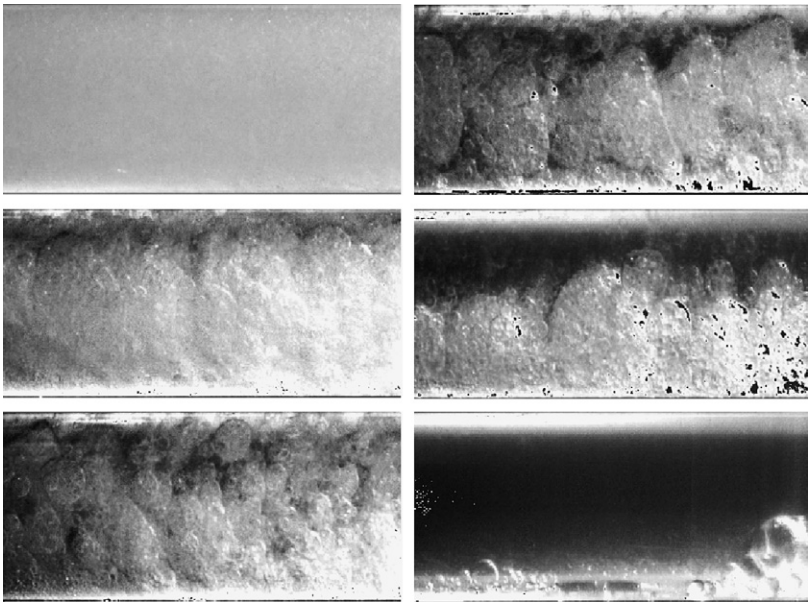

Fig. 5. A side view of the pipe during the inversion from a water-continuous flow to an oil-continuous flow during a continuous experiment. Starting from the top-left picture the center-left picture is taken after 6 s, the bottom-left picture after 22 s, the top-right picture after 33 s, the center-right picture after 38 s and the bottom-right picture after 77 s.

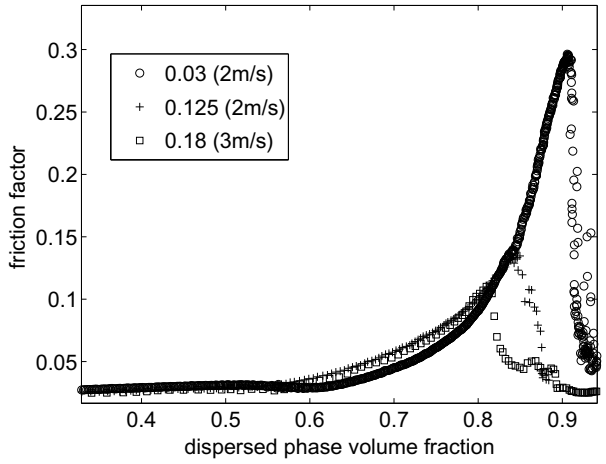

Fig. 6. Friction factor for water-to-oil continuous experiments for the following values of the injection phase volume fraction: 0.03; 0.125; 0.18. Mixture velocities of 2 and 3 m/s were used, but the results were independent of the mixture velocity.

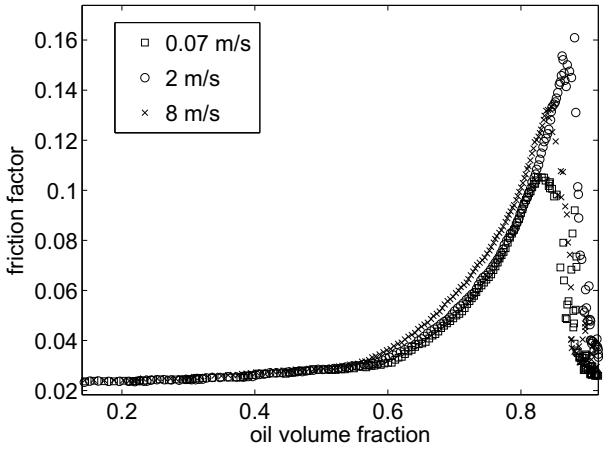

Fig. 7. Friction factor for water-to-oil continuous experiments at 2 m/s and injection phase volume fraction of 0.125 as function of the dispersed phase volume fraction for three values of the injection velocity (0.07 m/s, 2 m/s and 8 m/s). Inversion occurs at a volume fraction between 0.85 and 0.89.

Table 1
Dimensionless numbers for water-continuous – or oil-continuous experiments at different superficial velocities

Water	*Re*	*Fr*	*We*	
1 m/s	1.6×10^4	6.4	354	
2 m/s	3.2×10^4	25.5	1418	
3 m/s	4.8×10^4	57.3	3190	
1.34 m/s	2.1×10^4	11.4	637	Dispersed phase boundary – Brauner (2001)
Shell Macron EDM 110	*Re*	*Fr*	*We*	
2 m/s	0.7×10^4	25.5	1129	
3.5 m/s	1.1×10^4	78	3458	
1.35 m/s	0.4×10^4	11.6	515	Dispersed phase boundary – Brauner (2001)

For the calculation of the Froude number the density difference between water and oil is used and for the calculation of the Weber number the interfacial tension between the two liquids. "Dispersed phase boundary" indicates the transition from the dispersed flow pattern to another flow pattern according to Brauner (2001).

are not very dependent on the injection velocity at a constant value of χ.

In the literature it is sometimes stated that at inversion the friction factor and the dispersed phase volume fraction depend on *Re*, *Fr*, *We* and χ (see Deshpande and Kumar, 2003; Ioannou et al., 2005; Mira et al., 2003). We found that the dependence on *Re*, *Fr* and *We* disappears for sufficient large values of these parameters. This is very likely due to the fact that (at high values of *Re*) the turbulence in the pipe flow dominates the mixing between the two liquids. So for our experiments the results only depend on the injection phase volume fraction χ.

3.3. Friction factor and conductivity

During each continuous experiment the pressure drop was measured at three different positions along the pipe (see Section 2.2) and the local friction factor was calculated. Also the conductivity of the mixture was measured. The friction factor and the (dimensionless) conductivity for a water-to-oil experiment at a mixture velocity of 1 m/s (the mixture velocity was sufficiently large to sustain a dispersed flow regime) and a injection phase volume fraction of 0.125 are shown in Fig. 8. (Only measurements during the last stage of the inversion process are shown.) For each downstream location the time is shifted to the time at the inlet by using the mixture velocity. In this way it is possible to study the development in time of a certain flow structure.

As during the experiment oil is gradually added to the mixture, the dimensionless conductivity (1 for water and 0 for oil) is decreasing. The conductivity starts to oscillate at 270 s due to the creation of oil-continuous pockets with a lower conductivity than the water-continuous region. With further oil injection more and more oil-continuous pockets appear and the oscillations in conductivity increase. Around 320 s the conductivity rapidly decreases, because there are more oil-continuous regions than water-continuous regions and finally inversion takes place.

In Fig. 8 also the result for the friction factor as function of injection time is shown. Before inversion the friction factor at 2 m (p2) and at 5 m (p3) downstream of the injector are the same. So the flow is fully developed already at 2 m downstream from the injector. At 270 s after the start of oil injection the creation of oil-continuous pockets causes local regions with a higher effective viscosity and (as with the conductivity) oscillations in the friction factor occur. With further injection oil-continuous pockets in water-continuous regions and water-continuous pockets in oil-continuous regions become about the same in number and size, causing a high effective viscosity (as can be seen from the increase of the friction factor) and large pressure fluctuations (and hence large fluctuations of the friction factor).

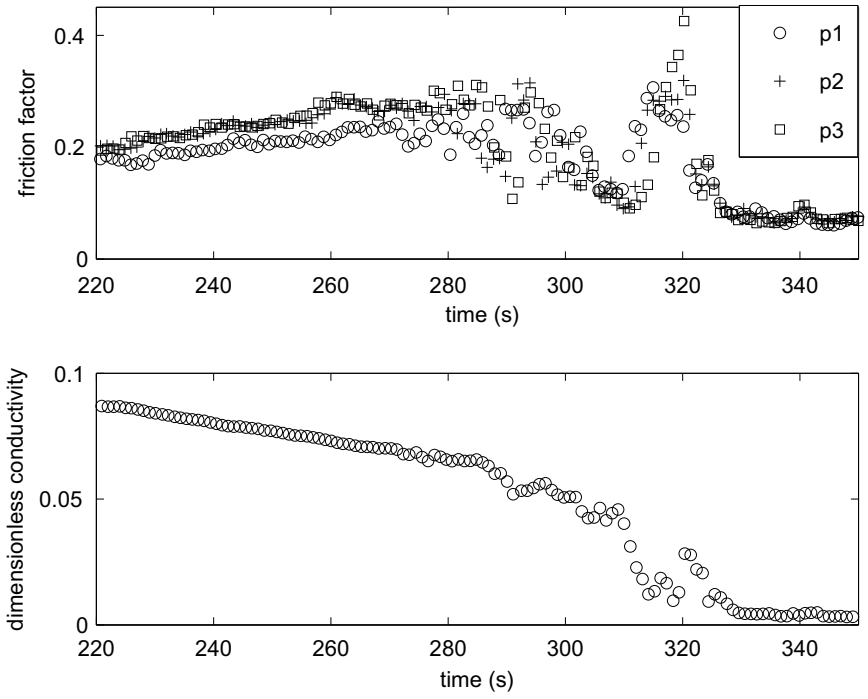

Fig. 8. Friction factor and dimensionless conductivity for a water-to-oil experiment at 1 m/s and injection phase volume fraction of 0.125 as a function of time.

At about 320 s after inversion the friction factor decreases and it seems as if the phase-inversion process has been completed. However, upstream of this large inverted region there is still a large non-inverted region (causing a high pressure and conductivity peak at about 320 s). It takes another passage through the injector (at this speed it takes the mixture 15 s for a complete cycle through the pipe loop) with additional oil injection to cause a phase inversion also in that region before the phase-inversion process is completed for the total pipe flow.

3.4. Critical concentration (dispersed phase volume fraction at inversion)

We have performed water-to-oil experiments and oil-to-water experiments for different mixture velocities. Water-to-oil experiments were carried out at mixture velocities of 1 m/s, 2 m/s and 3 m/s, and an oil-to-water experiment only at a mixture velocity of 3.5 m/s. (As oil is more viscous than water, the flow was for the oil-to-water experiment only at a velocity of 3.5 m/s sufficiently turbulent to make the results independent of the injection method.) For each mixture velocity it was found, that the volume fraction of the dispersed phase at inversion (the critical concentration) increases with decreasing injection phase volume fraction χ (see Fig. 9 and Piela et al. (2006)). This is likely due to the fact that with decreasing χ the flow is less disturbed and phase inversion is postponed to higher values of the dispersed phase volume fraction. For both cases (water-to-oil) and (oil-to-water) the critical concentration depends almost linearly on χ. Only for oil-to-water experiments at very low injection rates χ the inversion occurs at a somewhat higher oil volume fraction than expected based on a linear relationship. That is likely due to the creation of multiple drops (small droplets of the continuous phase in larger drops of the other phase), which increases the effective dispersed phase volume fraction. At low injection rates there is more time for the development of multiple drops (for more details see Piela et al., 2006 and Tyrode et al., 2003).

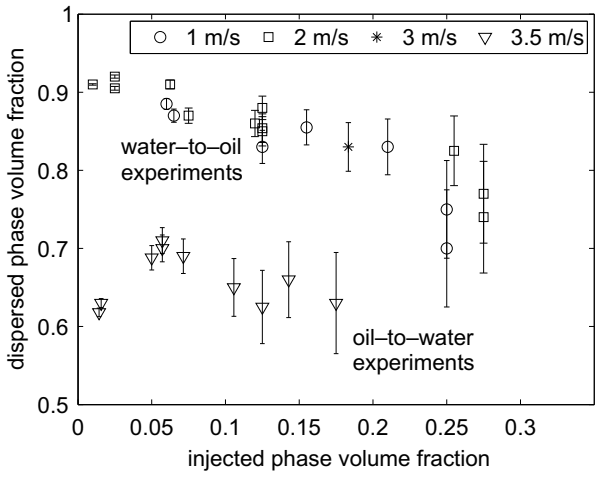

Fig. 9. Dispersed phase volume fraction at point of inversion as function of injection phase volume fraction χ and several values of the mixture velocity for water-to-oil experiments and oil-to-water experiments. Note that for water-to-oil experiments oil is the dispersed phase, whereas for oil-to-water experiments water is the dispersed phase.

4. Results for direct experiments

In a direct experiment the oil and water are simultaneously injected by means of two pumps into the pipe at a certain (constant) mixture fraction. Inside the pipe both liquids mix and the flow becomes water-continuous or oil-continuous dependent on the concentration of the two phases. Similar experiments in a horizontal pipe were carried out by Ioannou et al. (2005). They observed that at the point of phase inversion the pressure drop as well as the conductivity were very unstable. Pal (1993) observed a strong increase in effective viscosity at phase inversion during direct experiments in a pipe. The emphasis of our direct experiments was on the change in morphological structures at the point of inversion and how that change influences the pressure drop.

4.1. Phase-inversion mechanism

During a direct experiment the phase fractions were kept constant in time. Since the two phases are well mixed the dispersed phase volume fraction in the pipe is equal to the dispersed phase volume fraction at the point of injection at the entrance to the pipe loop. Close to the point where the flow changed from a water-continuous to an oil-continuous flow or vice versa, strong variations in the morphological structures of the dispersion were observed. For a mixture velocity of 2 m/s these changes occur at oil volume fractions between 0.5 and 0.6. Fig. 10 shows the dispersion morphology for three different values of the oil volume fraction. The top pictures show the dispersion at an oil volume fraction of 0.5. In the left top picture water is the continuous phase with (multiple) oil drops and oil pockets. In the right top picture there is an oil-continuous region at the top with water drops, and a water-continuous region at the bottom with (multiple) oil drops and oil pockets. At this oil volume fraction of 0.5 most of the flow is water continuous with some oil-continuous regions. At an oil concentration of 0.56 (see bottom-left picture) the flow consists of many (water-continuous) pockets in oil-continuous regions (dark regions), and (multiple) oil drops in water-continuous regions (see, for instance, center part of the picture). At a still higher concentration of 0.58 (see bottom-right picture) most of the flow field is oil continuous.

There is an important difference between a continuous experiment and a direct experiment. In a continuous experiment the inversion process starts with the coalescence of drops leading to the formation of larger drops, pockets and regions by encapsulation of parts of the continuous phase. Finally this process causes the disappearance of regions of the originally continuous phase. In a direct experiment the two liquids are mixed from the start at a constant concentration of the phases and there is no preliminary structure. Depending on the concentration, the liquids mix as a water-continuous mixture or an oil-continuous one. However, at a concentration of about 0.5–0.6 both water-continuous and oil-continuous regions are created during the same experiment (because of the non-homogeneous mixing, in particular in the *T*-junction and the entrance region of the pipe). At the concentration of around 0.5–0.6 none of the regions is sufficiently strong to dominate the other one, and so both regions flow downstream. These regions interact, entrap parts of the other continuous phase, break-up and coalescence (see Appendix A) causing a large pressure gradient over the pipe.

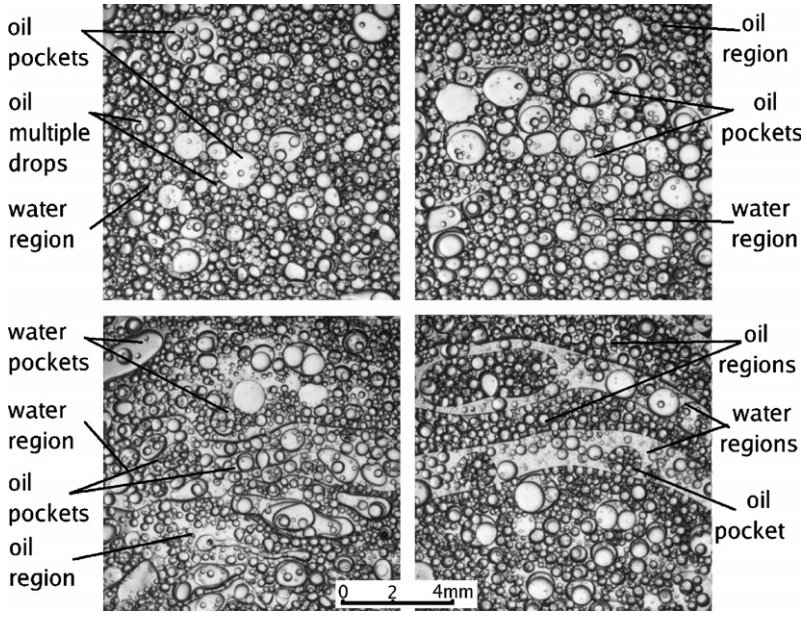

Fig. 10. Direct experiments at a mixture velocity 2 m/s. Pictures taken at different concentrations. Top-left and top-right pictures are taken at an oil volume fraction of 0.5, the bottom-left picture at 0.56 and the bottom-right picture at 0.58.

4.2. Friction factor and conductivity

At a low concentration of either of the two phases the friction factor and conductivity are for a direct experiment the same as for a continuous experiment. However, for a direct experiment with a concentration of around 0.5 for both phases an increase in the friction factor was observed and the conductivity started to oscillate. As discussed at such conditions strong interactions between oil-continuous regions and water-continuous regions take place, which cause a significant increase in the effective viscosity of the mixture (as can be concluded from the strong increase of the friction factor). The friction factor, dimensionless conductivity and oil volume fraction for a direct experiment at a mixture velocity of 3 m/s and an average oil volume fraction of 0.52 are shown in Fig. 11. The friction factor was determined for six different positions downstream of the injector. For each downstream location the time is again shifted to the time at the inlet by using the mixture velocity. Fig. 11 shows that just after the inlet (p1) the friction factor is nearly constant, as during the experiment the two liquids entered the pipe as separate layers and mixing of these layers still had to take place. Two meter downstream (p2) the friction factor is increasing, because the flow was developing and mixing had started. Five meter downstream (p3) the friction factor is already much higher and peaks are visible. Still further downstream (p4, p5 and p6) the peaks remain nearly the same. An interesting point is, that the peaks in the friction factor coincide with steep gradients of the conductivity. As can be seen in Fig. 11 the conductivity is changing because the oil volume fraction is not constant during the experiment (bottom graph in Fig. 11). The changing pressure in the inlet causes small oscillations in the oil volume fraction (the flow rate through the pumps is not completely stable). When the oil volume fraction is lower than 0.52, there are more water-continuous regions in the flow (conductivity value is closer to conductivity of water continuous flow). When the oil volume fraction is higher, there are more oil-continuous regions.

4.3. Critical concentration

It is hard to decide, what the critical concentration is in a direct experiment. At values of the oil volume fraction between 0.5 and 0.6 the flow is unstable, which means that oil-continuous regions and water-continuous regions coexist and interact flowing downstream. Fig. 12 shows the average (averaged over at least 40 s) friction factor for the three locations at p4, p5 and p6 for mixture velocities of 2 m/s and 3 m/s. It can be seen that at low and high oil volume fractions the friction factor is small and equal to the friction factor of the single phase (0.024 for pure water and 0.035 for pure oil at 2 m/s). The (average) friction factor has a maximum around an oil volume fraction of about 0.54. At this point the interaction between oil-continuous regions and water-continuous regions is strongest (effective dispersed phase fraction is highest, hence effective viscosity has a maximum). The width of the curve for the friction factor as function of the oil volume fraction seems more narrow for a mixture velocity of 3 m/s than for 2 m/s. The reason is likely, that at a higher velocity the interaction

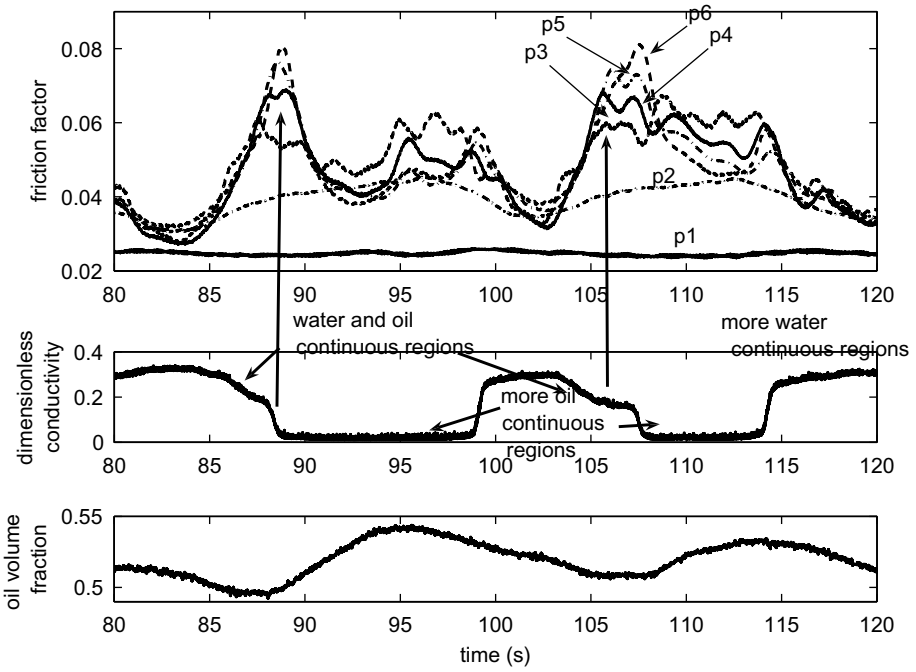

Fig. 11. Friction factor, dimensionless conductivity and oil volume fraction for direct experiment at mixture velocity of 3 m/s and an averaged oil volume fraction of 0.52. The time is shifted by using the average mixture velocity.

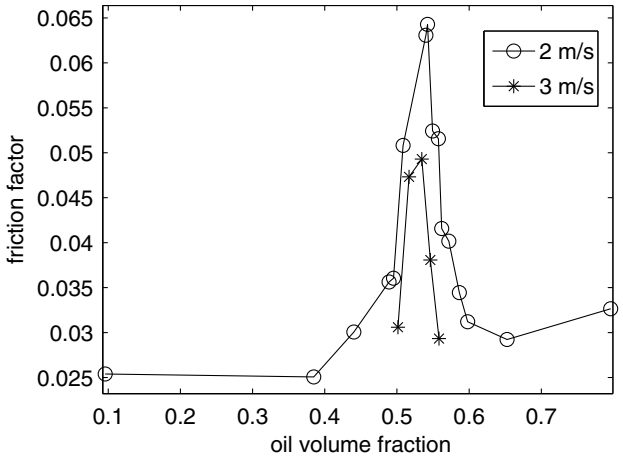

Fig. 12. Friction factor for direct experiment at mixture velocity of 2 m/s and 3 m/s as a function of oil volume fraction.

between oil continuous and water continuous regions is stronger. The mixing process is faster. So the strong increase in friction factor during this development period takes place over a shorter length of the pipe and the average friction factor over the complete length of the pipe is lower.

For a direct experiment one could argue, that there is no phase inversion comparable to the phase inversion in a continuous experiment. In a continuous experiments there is a constant injection of one of the phases. This causes an increase in the number of drops of the injected phase, which leads to the formation of pockets and regions of the injected phase due to coalescence. These pockets and regions of the injected phase start to interact with pockets and regions of the other phase, and with a further increase in the concentration of the injected phase inversion occurs. So the constant injection of one of the phases is crucial for phase inversion. In a direct experiment at an oil volume fraction between 0.5 and 0.6 water-continuous regions and oil-continuous regions are directly formed due to mixing of the phases downstream of the entrance to the pipe. So certain parts of the mixture flow are oil continuous and other parts water continuous. Below this critical concentration region between 0.5 and 0.6 the flow is always water continuous and above it the flow is always oil continuous (the measured conductivity does not fluctuate). The mixing of the two phases is crucial. However, in the concentration region between 0.5 and 0.6 the interactions between water-continuous regions and oil-continuous regions (leading to high friction factors and oscillations in conductivity) are very similar to the ones observed for a continuous experiment.

5. Drop interactions during phase-inversion process

In the preceding paragraphs we have given results for two types of experiments: the continuous experiment and the direct experiment. During both experiments there is a transition between a water-continuous phase and an oil-continuous phase (or vice versa). We will loosely call all these transition processes phase inversion, although one could argue that real phase inversion only occurs in a continuous experiment. During phase inversion there is strong interaction between water-continuous regions and oil-continuous regions. These regions have developed due to coalescence of drops and pockets (continuous experiment) and due to turbulent mixing of the originally separate phases (direct experiment). The interaction of the water-continuous regions and oil-continuous regions lead to a high effective viscosity and hence a large friction factor. In the appendix we discuss in some detail the coalescence, break-up and escape processes as observed during the experiments.

6. Discussion

As mentioned in the introduction many scientists studied the phase inversion process by means of stirred-vessel experiments. They found, for instance, that an ambivalence region exists. Dependent on the experimental conditions (turbulence level, presence of a surfactant, etc.) the flow can be oil continuous or water continuous (Tidhar et al., 1986; Arashmid and Jeffreys, 1980; Deshpande and Kumar, 2003). So the critical concentration at which phase inversion takes place, depends then on the experimental conditions.

In our pipe flow experiments we also paid attention to the region between the maximum and minimum value of the dispersed phase fraction where phase inversion can take place (for a certain set of conditions). During the continuous experiments we found that the critical volume fraction of the dispersed phase at the point of inversion is not so much dependent on *Re*, *Fr*, *We* and also not on the injection velocity of the dispersed phase, as long as the mixture velocity is sufficiently large ($\geqslant 2$ m/s). However, we found that the injection phase volume fraction χ had a significant influence on the critical concentration. This makes it possible to represent the critical volume fraction as measured during the experiments as function of χ (see Fig. 13). The upper line gives the oil volume fraction at the point of phase inversion as measured during water-to-oil continuous experiments; the lower line represents the oil volume fraction at inversion measured during oil-to-water continuous experiments. The region in between the two lines is the ambivalence region, where both oil and water can be the continuous phase (depending on the 'history' of the experiment). As can be seen the width of the ambivalence region decreases with increasing injection phase volume fraction χ. The direct experiment can be considered as the limiting case of a continuous experiment, with a large injection rate of the dispersed phase and with inversion taking place before one cycle through the pipe loop is completed. The injected phase volume fraction is then equal to the ratio of the injected volume rate of one of the two phases to the volume rate of the mixture. The phase with the lowest

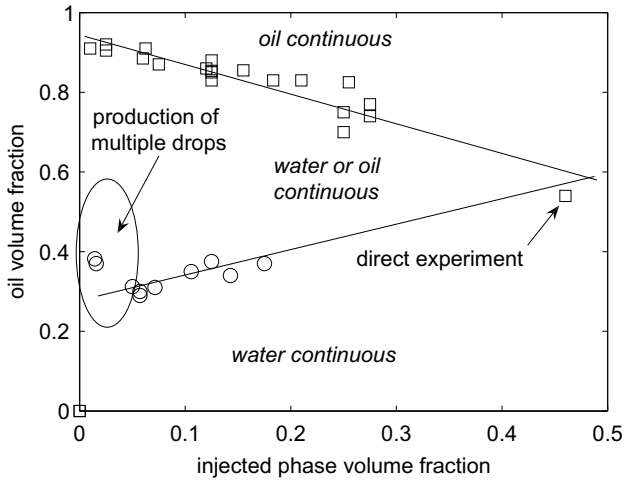

Fig. 13. Inversion map. The upper line gives the oil volume fraction at the point of inversion as measured during water-to-oil continuous experiments. The lower lines represents the oil volume fraction at inversion as measured during oil-to-water continuous experiments. The region in between the two lines is the ambivalence region, where both oil and water can be the continuous phase. Also the oil volume fraction at inversion as measured during the direct experiments is indicated.

volume rate is considered as the injected phase. As can be seen in Fig. 13 with this interpretation the measured critical concentration at inversion for the direct experiment fits well with the results of the continuous experiments.

As indicated before during the oil-to-water experiments the formation of multiple drops (oil droplets in water drops in a continuous phase of oil) was found. Due to the inclusion of water droplets in the oil drops the effective dispersed phase volume fraction is larger than as calculated starting from the assumption that only pure oil drops are present. This effect explains the deviation of the measured critical volume fraction for the oil-to-water experiments at low values of χ. (This effect was found to be unimportant for water-to-oil experiments. Multiple drops consisting of water droplets in oil drops in a continuous phase of water were very unstable and did not live long.)

7. Conclusions

An important conclusion of our work is, that also for pipe flows the critical concentration can be significantly higher for continuous experiments than for direct experiments. By careful injection of the dispersed phase during continuous experiment phase inversion can be postponed to very high values of the dispersed phase volume fraction. For practical applications this result is important, as it opens the opportunity to avoid or postpone phase inversion (causing a high pressure drop or low flow rate).

Another conclusion of our work is that although the critical volume fraction of the dispersed phase at phase inversion was found to be very different for the two types of experiments, the change in morphological structures was always the same. Far away from the point of inversion the dispersed phase consists of (nearly) spherical drops. However close to inversion the situation changes drastically. Larger morphological structures appear in the form of pockets and regions of the dispersed phase. With increasing dispersed phase volume fraction the concentration of these isolated pockets and regions of the (originally) dispersed phase becomes so high, that they coalesce at certain places in the flow field where isolated pockets and regions of the (originally) continuous phase are formed. With a further increase in volume fraction of the (originally) dispersed phase the balance between the two types of pockets and regions changes in such a way, that the (originally) dispersed phase becomes the continuous one and the (originally) continuous phase the dispersed one. With a still further increase in volume fraction the dispersed phase consists again of (nearly) spherical drops.

Acknowledgements

The authors are grateful to Shell Exploration and Production and FOM (Foundation for Fundamental Research on Matter in The Netherlands) for the financial support to this project.

Appendix A. Drop interactions during phase-inversion process

During our experiments we observed three types of drop interactions: coalescence, break-up and escape.

- Coalescence occurs when two units (drops, pockets or regions) stay in contact for a sufficiently long time. The film between them ruptures and a larger unit is created. Fig. A.1 shows two examples of coalescence. On the left-hand side a large (multiple) drop and a region can be observed (top-left picture). After 0.01 s the multiple drop and region collide (center-left picture). After only 0.016 s (bottom-left picture) they have merged and a new surface is created. Remains of the multiple drop are now present inside the region. On the right-hand side an elongated region collides with another region. The top-right picture shows them before collision. The center-right picture was taken after 0.004 s and the regions have already almost completely merged. The bottom-left picture shows the situation after 0.008 s. Another form of coalescence between two regions occurs, when a part of one of the regions is entrapped in form of a drop in the other region. Fig. A.2 shows two examples of entrapment. On the left side a water-continuous region is enclosed between two oil-continuous regions (top-left picture). The water-continuous region elongates (second picture from the top on the left-hand side, taken after 0.004 s) and becomes eventually so thin, that coalescence between the two oil continuous regions occurs (third picture from the top on the left-hand side, taken after 0.006 s). That leads also to entrapment of part of the water-continuous region

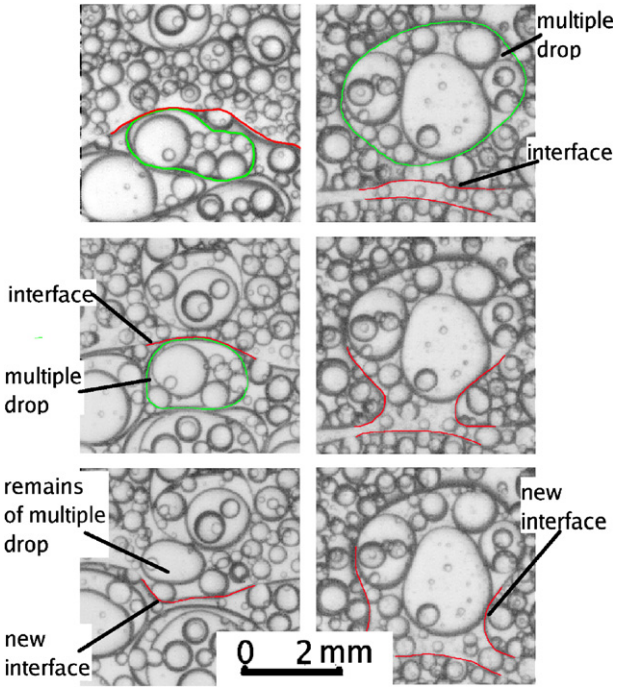

Fig. A.1. Two examples of coalescence between a multiple drop and a region.

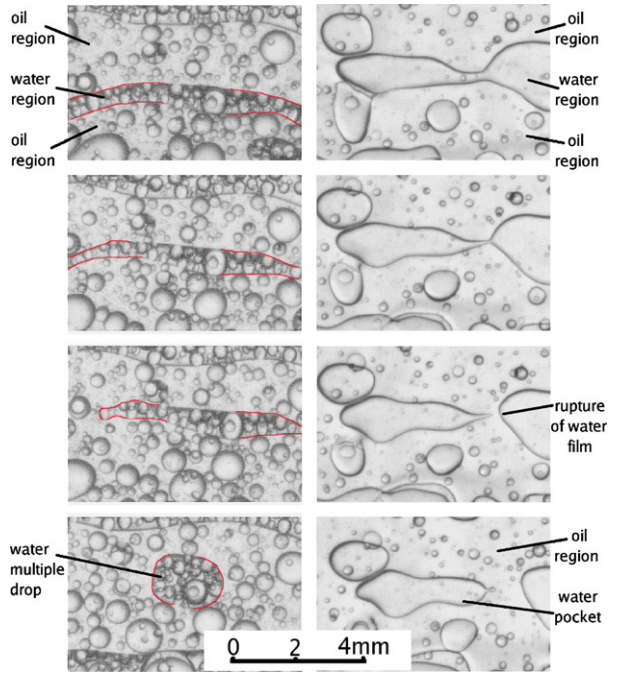

Fig. A.2. Two examples of coalescence which leads to entrapment.

inside the new oil-continuous region (bottom-left picture, taken after 0.016 s). On the right-hand side of Fig. A.2 the process of entrapment of a part of a water-continuous region inside an oil-continuous region is shown. After 0.004 s (second picture from the top on the right-hand side) the thickness of the water film is decreasing. After 0.006 s (third picture from the top on the right-hand side) it breaks and merging of the two oil regions occurs. And after 0.01 s (bottom-right picture) part of the water-continuous region is entrapped as a water pocket inside the new extended oil-continuous region.

- Break-up occurs when the fluctuating hydrodynamic force on the surface of a drop or pocket exceeds the surface tension. Fig. A.3 shows the break-up of two pockets. The top picture shows two elongated pockets. The pocket on the right-hand side breaks after 0.004 s. The pocket on the left-hand side is further elongated and breaks after 0.008 s.
- Escape occurs when the film between an entrapped drop or pocket present inside a certain region and another outside region breaks. Fig. A.4 shows the escape of a multiple drop into an outside region. The top-left picture shows the structure before the escape process starts. After 0.002 s (bottom-left picture) the film ruptures. After 0.004 s (top-right picture) droplets originally present inside the multiple drop have been released into the outside region. After 0.006 s (bottom-right picture) also

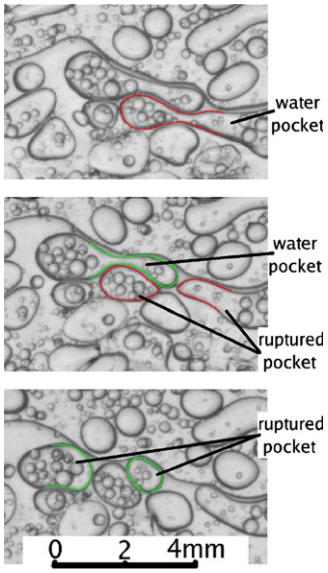

Fig. A.3. Break-up of the multiple drop.

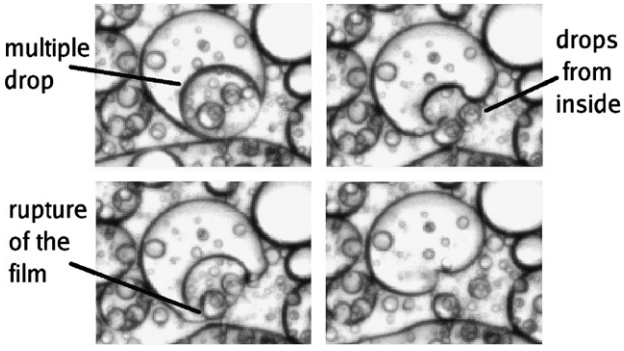

Fig. A.4. Escape of the multiple drop from the region.

the surface of the inner region is adapting to the new condition.

References

Arashmid, M., Jeffreys, G., 1980. Analysis of the phase inversion characteristics of liquid–liquid dispersions. AIChE J. 26.

Becher, P., 2001. Emulsions: Theory and Practice. Oxford University Press.

Binks, B., Lumsdon, S., 2000. Catastrophic phase inversion of water-in-oil emulsions stabilized by hydrophobic silica. Langmuir 16, 2539–2547.

Brauner, N., 2001. The prediction of dispersed flows boundaries in liquid–liquid and gas–liquid systems. Int. J. Multiphase Flow 27, 885–910.

Brauner, N., Ullmann, A., 2002. Modeling of phase inversion phenomenon in two-phase pipe flows. Int. J. Multiphase Flow 28, 1177–1204.

Chakrabarti, D., Das, G., Das, P., 2006. The transition from water continuous to oil continuous flow pattern. AIChE J. 52, 3668–3678.

Deshpande, K., Kumar, S., 2003. A new characteristic of liquid–liquid systems – inversion holdup of intensely agitated dispersions. Chem. Eng. Sci. 58, 3829–3835.

Dickinson, E., 1981. Interpretation of emulsion phase inversion as a cusp catastrophe. J. Colloid Interf. Sci. 84, 284–287.

Groeneweg, F., Agterof, W., Jaeger, P., Janssen, J., Wieringa, J., Klahn, J., 1998. On the mechanism of the inversion of emulsions. Trans IChemE 76 Part A.

Ioannou, K., Nydal, O., Angeli, P., 2005. Phase inversion in dispersed liquid–liquid flows. Exp. Thermal Fluid Sci. 29, 331–339.

Liu, L., Matar, O., Lawrence, J., Hewitt, G., 2006. Laser-induced fluorescence (lif) studies of liquid–liquid flows. Part i: flow structures and phase inversion. Chem. Eng. Sci. 61, 4007–4021.

Liu, L., Matar, O., Perez de Ortiz, E., Hewitt, G., 2005. Experimental investigation of phase inversion in a stirred vessel using lif. Chem. Eng. Sci. 60, 85–94.

Mira, I., Zambrano, N., Tyrode, E., Márquez, L., Pena, A., Pizzino, A., Salager, J., 2003. Emulsion catastrophic inversion from abnormal to normal morphology. 2. Effects of the stirring intensity on the dynamic inversion frontier. Ind. Eng. Chem. Res. 42, 57–61.

Náďler, M., Mewes, D., 1997. Flow induced emulsification in the flow of two immiscible liquids in horizontal pipes. Int. J. Multiphase Flow 23, 55–68.

Pacek, A., Nienow, A., 1995. A problem for the description of turbulent dispersed liquid–liquid systems. Int. J. Multiphase Flow 21, 323–328.

Pacek, A., Nienow, A., Moore, I., 1994. On the structure of turbulent liquid–liquid dispersed flows in an agitated vessel. Chem. Eng. Sci. 49, 3485–3498.

Pal, R., 1993. Pipeline flow of unstable and surfactant-stabilized emulsions. AIChE J. 39, 1754–1764.

Pal, R., 2000. Shear viscosity behavior of emulsions of two immiscible liquids. J. Colloid Interf. Sci. 225, 359–366.

Piela, K., Delfos, R., Ooms, G., Westerweel, J., Oliemans, R., Mudde, R., 2006. Experimental investigation of phase inversion in an oil–water flow through a horizontal pipe loop. Int. J. Multiphase Flow 32, 1087–1099.

Quinn, J., Sigloh, D., 1963. Phase inversion in the mixing of immiscible liquids. The Can. J. Chem. Eng. 15–18.

Rondón-Gonzaléz, M., Sadtler, V., Choplin, L., Salager, J., 2006. Emulsion catastrophic inversion from abnormal to normal morphology. 5. Effect of the water-to-oil and surfactant concentration on the inversion produced by continuous stirring. Ind. Eng. Chem. Res. 45, 3074–3080.

Sajjadi, S., Jahanzad, F., Yianneskis, M., Brooks, B., 2003. Phase inversion in abnormal o/w/o emulsion. 2. Effect of surfactant hydrophilic–lipophilic balance. Ind. Eng. Chem. Res. 42, 3571–3577.

Sajjadi, S., Zerfa, M., Brooks, B., 2000. Morphological change in drop structure with time for abnormal polymer/water/surfactant dispersions. Langmuir 16, 10015–10019.

Sajjadi, S., Zerfa, M., Brooks, B., 2002. Dynamic behaviour of drops in oil/water/oil dispersions. Chem. Eng. Sci. 57, 663–675.

Smith, D., Lim, K., 1990. An experimental test of catastrophe and critical-scaling theories of emulsion inversion. Langmuir 6, 1071–1077.

Tidhar, M., Merchuk, J., Sembira, A., Wolf, D., 1986. Characteristics of a motionless mixer for dispersion of immiscible fluids – ii. Phase inversion of liquid–liquid systems. Chem. Eng. Sci. 41, 457–462.

Tyrode, E., Allouche, J., Choplin, L., Salager, J., 2005. Emulsion catastrophic inversion from abnormal to normal morphology. 4. Following the emulsion viscosity during three inversion protocols and extending the critical dispersed-phase concept. Ind. Eng. Chem. Res. 44, 67–74.

Tyrode, E., Mira, I., Zambrano, N., Márquez, L., Rondón-Gonzaléz, M., Salager, J., 2003. Emulsion catastrophic inversion from abnormal to normal morphology. 3. Conditions for triggering the dynamic inversion and application to industrial processes. Ind. Eng. Chem. Res. 42, 67–74.

Vaessen, G., Visschers, M., Stein, H., 1996. Predicting catastrophic phase inversion on the basis of droplet coalescence kinetics. Langmuir 12, 875–882.

Yeo, L., Matar, O., Perez de Ortiz, E., 2002. A simple predictive tool for modelling phase inversion in liquid–liquid dispersions. Chem. Eng. Sci. 57, 1069–1072.